Chapter 4

# Dependent and Independent Parameters of Needleless Electrospinning

Fatma Yalcinkaya , Baturalp Yalcinkaya and Oldrich Jirsak

Additional information is available at the end of the chapter

http://dx.doi.org/10.5772/65838

**Abstract**

Electrospinning is a simple method to produce nanofibers from solutions and melt of different polymers and polymer blends. There is an extensive application in future of Electrospun nanofibers. Several methods for the production of nanofibers have been developed for their wide-scale production. In this chapter, we introduced the needleless roller electrospinning system that is well known under the trade name of nanospider and used as industrial production scale during the last decade. For industrial production, it is crucial to control and the measure all the spinning parameters of the needleless electrospinning system. Herein, all the electrospinning parameters of the needleless roller electrospinning system were determined and grouped as dependent and independent parameters. Each parameter was defined, and some experimental results are shown under their group. Using theoretical calculations, the minimum electrical field to start initiation of Taylor's cone and the dimensionless electrospinning number was demonstrated. The dimensionless electrospinning number is important for the initiation of the electrospinning system. Each parameter explained in detail, and measurement methods of parameters were clarified. It was found that each parameter plays a major role in productivity and quality of nanofiber webs. Changing the dependent and independent parameters of the electrospinning, the fiber morphology can be adjusted according to demands.

**Keywords:** roller electrospinning, parameters, nanofiber, needleless electrospinning

## 1. Introduction

Electrospinning is a versatile method to produce ultra-thin fibers less than 1 μm. Nanofibers produced from electrospinning have enormous properties such as high surface area, highly pore structure, small pore size, and electrical properties, and so on. Based on specific properties of nanofibers, scientists focus on a promising application area of nanofibers. Nanofibers can be used for filtration, wound dressing, drug delivery, tissue engineering, artificial vessels, barrier textiles, sensors, carriers, and so on [1–4]. Electrospinning methods can be grouped into two: needle and needleless electrospinning. There are system and process parameters that have an effective role on the morphology of nanofibers. Process parameters can be defined as needle diameter, distance between electrodes, feed rate, applied voltage, ambient conditions while system parameters can be defined as polymer solution properties such as surface tension, viscosity, molecular weight, and solvent for the needle electrospinning system. Unlike the single needle electrospinning system, needleless electrospinning is useful equipment for significant bulk production in an industrial scale. Niu and Lin grouped the needleless electrospinning system as upward and downward [5]. One of the most popular upward needleless electrospinning systems is a roller electrospinning system that was developed by Jirsak et al. [6]. Despite many types of research about parameters of needle electrospinning, there is not enough information about needleless electrospinning.

The parameters of needleless roller electrospinning can be divided into two groups: dependent and independent. Each parameter has an influence on the resultant fiber morphology and spinnability. Cengiz and Jirsak [7] and Yener et al. [8] showed that the addition of tetraethylene ammonium bromide (TEAB) salt increases the spinning performance and resultant fiber diameter of polyurethane (PU) nanofibers. In another work, it was found that increasing the humidity of the spinning unit at a constant temperature, the spinning performance altered for polyvinyl alcohol (PVA) nanofibers while the nonfibrous area increases with humidity. On the other hand, at constant relative humidity, upon the increasing temperature from 20 to 30°C the spinning performance decreases almost three times so do the fiber diameter and nonfibrous area [9].

In this chapter, we focus on roller electrospinning and parameters. Independent parameters are the parameters that can be changed before or during spinning while dependent parameters are resultant parameters of independent ones. These parameters are explained in the next section. This work is a part of the Ph.D.thesis, the experimental and theoretical results were studied in detail in reference [10].

## 2. Principle of needleless electrospinning

Two common methods have been utilized for the production of nanofibers which are needle electrospinning and needleless electrospinning from a free surface. Both the spinning techniques were explained in the previous work [11]. The mechanism and the principle of the needle

electrospinning system were explained deeply in the literature whereas there is not enough information about free surface needleless electrospinning.

Tonks [12] studied on the mechanism for the onset of aperiodic instability ($\omega^2 < 0$) of the free surface when subjected to a strong electric field. The initial perturbation of the surface causes a localfield increase which determines the further growth of the perturbation. The critical field is determined directly from the corresponding dispersion equation [13];

$$\omega^2 = \frac{k}{\rho}\left(\sigma k^2 + \rho g - \frac{E^2}{4\pi}k\right) \tag{1}$$

where $g$ is the gravitational acceleration, $\sigma$ is the surface tension, $\rho$ is the density, $E$ is electrical field strength, $k = 2\pi/\lambda$ is the wave number, and $\lambda$ is the wavelength.

Lukas et al. explained the fasting-forming instability mechanism [14]. In the principle, the capillary waves on a one-dimensional approach of the liquid surface are used to analyze the electrohydrodynamics. The vertical displacement of the wave was calculated by the periodic real part of a complex quantity, $\xi = A \exp[i(kx - \omega t)]$. The $A$, $k$, and $\omega$ are amplitude, wave number, and angular frequency, respectively. The wave number ($k$) can be calculated using the wavelength ($\lambda$), $k = 2\pi/\lambda$. The relationship between the angular frequency $\omega$ and the period $T$ is $\omega = 2\pi/T$ [10].

The relationships $\omega = f(k)$ between spatial and time-dependent parameters $k$ and $\omega$ of waves undergoing various force fields that are called dispersion laws. For gravity waves, $\omega^2 = gk$, where $g$ is gravity acceleration. By adding surface tension:

$$\omega^2 = (\rho g + \gamma k^2 - \varepsilon E_0{}^2 k)\frac{k}{\rho} \tag{2}$$

where $\rho$ is liquid mass density, $\gamma$ is a linear force of surface tension, $k$ is wave number, $\varepsilon$ is permittivity, and $E_0$ is field strength.

Lukas also gives out a new concept that is dimensionless electrospinning number $\Gamma$ [15]. The dimensionless electrospinning number is the ratio of electric pressure ($Pe$) to capillary pressure ($Pc$). So we have, $\Gamma = Pe/Pc$. Capillary pressure ($Pc$) caused by an arbitrarily curved liquid surface is a product of the surface tension and a sum of two principal curvatures $K1$ and $K2$, so $Pc = \gamma(K1 + K2)$.

In the case of the sphere with a radius $Rs$ in a gravitational acceleration field, both principal curvatures $K1$ and $K2$ are of the same value and are equal to $1/Rs$, so $Pc = 2\gamma/Rs$.

Electric pressure ($Pe$) is another basic concept in electrospinning, and it is calculated according to Eq. (3);

$$Pe = \left(\varepsilon E^2\right)/2 \tag{3}$$

where $E$ is the strength of electric field and $\varepsilon$ is the permittivity of surrounding air.

So, the phenomenon of electrospinning only occurs when the dimensionless electrospinning number is bigger or at least equal to 1 ($\Gamma \geq 1$ or $Pe \geq Pc$).

In the needle electrospinning, the polymer solution is drawn into fibers in electrostatic field arranged between a needle tip and a collector. Polymer solution stretches into fibers while the solvent is evaporating. Fibers in nanorange or microrange are collected on a collector. Fiber quality and morphology depend on several factors. The morphology of nanostructures formed on the collector varies with parameters of the spinning device and process parameters [10].

Dao et al. divided electrospinning processes into three stages: in the first stage, the polymer solution is fed by a roller from the container or by the pump. High electric potential inserted in the solution leads to the formation of jets. The jets (jet) are discharged from roller's surface Or droplet on the needle tip. As a result, the jets accelerate steadily and thin out along an axis aligned with the general direction of the electric field. It is a critical stage because the first stage is the key for the controlling subsequent stages and effects of the final fiber properties. In the second stage, several processes are forming simultaneously such as electric line fluctuation as a result of time and the space variation in the bulk density of charges causes jets to turn transversely to the field direction and to be decelerated by the constantly increasing drag force of the gas. A cloud is produced that expands toward the collector by the action of the same-polarity charges. At the same time, the rate of vaporization of the solvent which started already at the first stage of the process is steeply intensified; the jet solidifies, and the resulting fibrous cloud drifts in the applied electric field onto the collector. During this stage, an unsteady bulk fiber web structure can be observed due to possible splitting of the jet. In the third stage, there are two simultaneous processes: random deposition of the nanofibers onto a substrate on the collector and the gas spark discharge between the collector and the fiber layer formed on it, that closes the electric circuit [16].

## 3. Technology and parameters of roller electrospinning

The roller electrospinning has been developed and patented at the Technical University of Liberec [6]. The roller electrospinning system is a highly productive method to produce nanofibers. In this method, there is a roller electrode that is immersed in a solution tank and a motor connected to the roller for rotation. The roller electrospinning system is a closed system; there is only input for air and humidity and output for air suction. On the top there is a collector (charged or grounded), and a conveyor material (generally nonwoven or paper) is passing through the collector as shown in **Figure 1** [17]. Nevertheless, its productivity is still low in comparison with processes yielding planar fibrous materials, and the price of nanofiber layers is correspondingly high. Therefore, further development based on the knowledge of the process is necessary to improve quality, regularity, and price of

http://dx.doi.org/10.5772/65838

nanofibers. The roller electrospinning can process a broad range of polymers in diameters of 50–800 nm with acceptable narrow fiber diameter distribution on nonwoven webs.

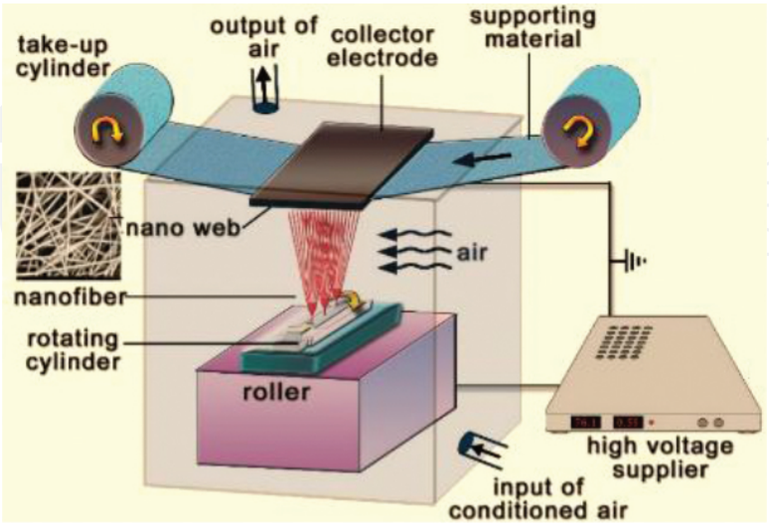


**Figure 1.** Schematic diagram of the roller electrospinning system.

| Independent parameters | Dependent parameters |
|---|---|
| • Polymer solution properties (concentration, viscosity, composition, surface tension, conductivity, molecular weight) | • Number of cones, density of jets |
| • Applied voltage | • Lifetime of jets |
| • Distance between electrodes | • Spinning performance, spinning performance/per jet |
| • Velocity or rotating roller | • Total average current, current/jet |
| • Velocity of take-up fabric | • Thickness of polymer solution layer on the surface of the roller |
| • Geometry of electrode | • Force acting on a jet |
| • Geometry of collector | • Spinning area |
| • Ambient conditions (temperature, relative humidity) | • Distance between neighboring jets |
| | • Jet length in stable zone |
| | • Fiber diameter and distribution |
| | • Nonfibrous area |
| | • Launching time of jets |

**Table 1.** Parameters of roller electrospinning system.

The electrospinning parameters are divided into two groups: namely independent and dependent ones. In the group independent parameters, primary and secondary independent parameters are distinguished, for instance kind of polymer, its molecular weight, kind of solvent, type and amount of additives, and concentration of polymer solution are primarily independent parameters, whereas viscosity, conductivity, and surface tension, as a result of

above parameters, directly influencing the electrospinning process, are secondary independent parameters [10].

The parameters of the roller electrospinning system were tabulated in **Table 1** [10].

### 3.1. Independent parameters

#### *3.1.1. Polymer solution properties*

##### *3.1.1.1. Concentration/molecular weight/viscosity*

Polymer jets must show some level of strength to create nanofibers during electrospinning. If the strength is too low, the jets break and create beads instead of fibers. Shenoy et al. [18] introduced the term "entanglement number" as a quantity responsible for the strength of jets. They also found the limiting value of an entanglement number regarding fiber production; if the value is greater than 3.5, fibers are produced, below 3.5 the production of beads starts. The entanglement number depends on the kind of polymer, namely on the content of polar groups and molecular weight, on the type of solvent and polymer concentration in the solution. As the determination of the entanglement number is not easy, the viscosity is often taken as a measure of it, as its principle depends on the same parameters as entanglement number. In a suitable concentration, the chain entanglements of macromolecules are adequate to electrospin a polymer into fibers under a strong electrostatic field.

The polymer solution viscosity is determined by such molecular interactions, either attractive or repulsive, and can be altered by changing the solvent type. The viscosity of polymer solutions depends on shear rate and temperature, it also depends on the molecular weight distribution and the concentration. Properties of solvents are affecting the chain entanglement. In a good solvent, the polymer swells and its volume increases. The intermolecular forces between the monomer and solvent subunits dominate over intramolecular interactions. In a bad solvent or poor solvent, intramolecular forces dominate and the chains contract. In theta-solvent, the intermolecular polymer-solvent repulsion balances exactly the intramolecular monomer-monomer attraction [19]. In aqueous, the overall shape of the chain will be affected by the amount of electrolyte (salt) in the solvent. In the absence of electrolyte, the charges are unshielded and repel each other. As a result, the chain is stretched out. However, when the electrolyte is present in the solution, the charges are shielded, and their effect is suppressed. As a result, the chain tends to shrink toward its original random configuration. This change from a rod to a sphere obviously causes the viscosity to decrease [20].

With the increasing concentration of polymer solutions prepared by using polymers with different molecular weights, the viscosity of polymer solutions was found to increase due to the densely entangled polymer chains [21]. A certain amount of chain entanglement is needed to keep the solution jet coherent during the electrospinning process. The high viscosity or the concentration of the solution prevents the jet to breakup into droplets. Moreover, the increase in chain entanglements results in an increase of viscoelastic force, which can be enough to prevent breakup of the electrically charged jet. As a result, the charged jet elongates through

a collector by Coulombic stress and the diameter of jet decreases [22]. With any further increase in the concentration (or viscosity) of the solution, the number of beads along the fibers was found to decrease, and their shape appeared to be more elongated [23]. The relationship between polyvinyl butyral nanofiber surface morphology, molecular weight and concentration are shown in **Figure 2**.

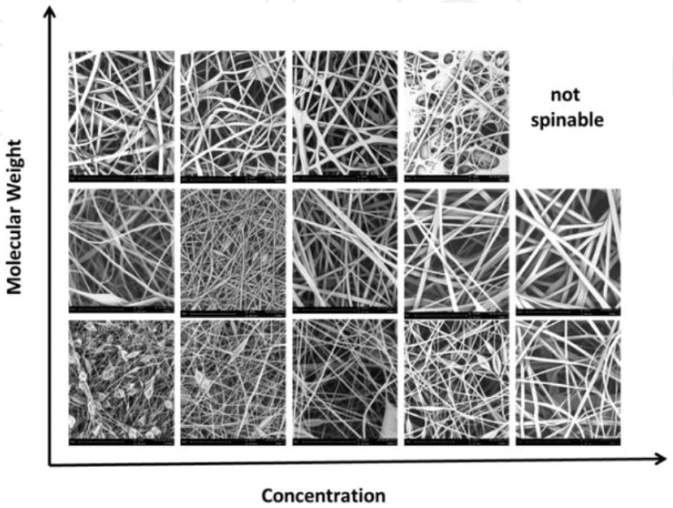


**Figure 2.** The relationship between the surface morphology of nanofibers, molecular weight, and concentration.

Cengiz et al. [24] studied the effect of PVApolymer molecular weight and some solution properties such as conductivity, surface tension, and rheological behaviorconcerning spinnability, process performance, fiber diameters, diameter distribution, and nonfibrous particles. It was found that electric conductivity and surface tension of the solutions did not influence both spinning performance and fiber diameter significantly, whereas molecular weight has an important effect on the spinnability. On the contrary, the concentration changes the process throughput considerably and properties of nanofibers and nanofiber layers to some extent.

In general, the relation between molecular weight, viscosity, and concentration, the number of entanglements per chain increases with molecular weight while entanglement per unit volume increases with concentration. In the previous studies, it was found that increasing concentration increases viscosity, and as a result, more polymer solution is transferred per one jet. Therefore, fabric throughput and fiber diameter increase [7, 16].

*3.1.1.2. Surface tension*

Surface tension tends to decrease the surface area per unit mass (and the surface energy) of fluid. If the electrostatic force overcomes the surface tension, a charged jet of a polymer solution is ejected. So, for a higher surface tension, a stronger electric field is required. Surface tension is related to the interaction between the molecules of polymer and solvent in solutions.

Fong et al. found that the number of beads decreased with increasing viscosity and net charge density and it also decreased with decreasing surface tension coefficient of the solutions [25].

Surface tension causes the solvent molecules to form spherical shape and aggregate when the free solvent molecules are in high concentration. The interaction between the polymer and the solvent molecules is high at high viscosity and results in the elongation of the solution under the electrical field. As a result of the electrical field, the solvent molecules will spread out from the polymer molecules and reduces the gathering of the solvent molecules under the effect of the surface tension.

**Figure 3** shows the PVA solution at various surface tension resulting in changes in fiber surface morphology. Nonionic surfactant was used not to change conductivity.

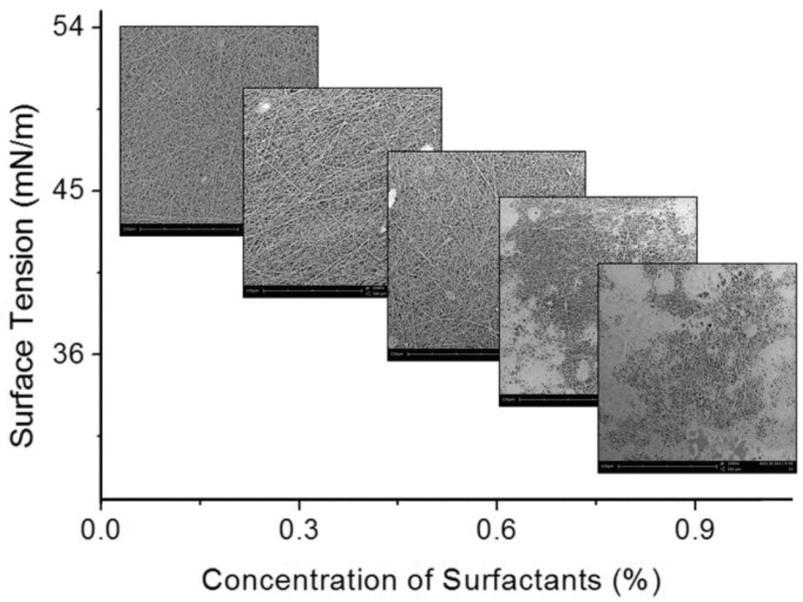


**Figure 3.** Effect of surface tension on the surface morphology of nanofibers.

*3.1.1.3. Conductivity and permittivity*

The electrospinning process operates due to the external electric field, the viscoelastic force due to the viscosity of the solution, surface tension force, conductivity, etc. The electric field between the electrode and the collector causes the solution to stretch. If the electrostatic field overcomes the surface tension, the nanofibers are formed. The stretching of the electrospun jet and the bending instability is mainly controlled by the Coulombic force between charges and the electric field. These forces arise due to the surface charge on the jet which can be varied by changing the conductivity of the solution. The increased charge carrier causes the jet to elongate and can produce uniform fibers with a smaller diameter. A higher net charge density of the polymer solution could, therefore, yield thinner fibers with no beads. Filatov et al. found that the acceptable range of conductivity in electrospinning is rather wide from $10^{-6}$ to $10^{-2}$ $(\Omega\ m)^{-1}$, where the upper limit is governed by the threshold of initiation of the gas discharge from the jet that destabilizes it. It was also discussed that the conductivity is associated with relative dielectric permittivity which usually varies little from its value of

the solvent that is used. The lower the permittivity, the lesser the attenuation of the electric field inside the nascent liquid jet and the higher the rate of electric charge transfer in the solution. However, decreasing of the polarity of solvent molecule reduces the extent of dissociation in it of ionogenic substances with a concurrent reduction in electrical conductivity. For the electrospinning process, the best values of relative permittivity were found to be between 5 and 30, with a limit not exceeding 100 [26]. The conductivity of the solution is the factor that determines the current and fiber diameter. The solution with high conductivity can carry more charge on the jet. Kim et al. found that nanofibers with the smallest fiber diameter can be obtained from the solution with the highest conductivity [27]. On the other side, Heikkila and Harlin found that at the same viscosity, polyacrylonitrile (PAN)/salt solution produced slightly larger fibers because increased conductivity enhanced the mass flow. The higher conductivity of the PAN/salt solution increased the instabilities in the electrospinning process [28].

It is common to use salt in polymer solutions to increase their conductivity. According to a previous work, the addition of salt to polymer solution such as polyurethane and polyvinyl butyral (PVB)enhances the number of jets on the roller surface and as a result the productivity increases [7, 29]. On the contrary, in the case of some other polymers such as polyethylene oxide (PEO) and PVA, the addition of salt decreases the spinning performance [30, 31]. This case can be explained by the leaky dielectric model that was first proposed by Melcher and Taylor [32].

### *3.1.2. Applied voltage*

It was investigated that a drop of liquid having surface tension $\gamma$, held at the end of a capillary tube of radius $r_0$, and raised to a potential difference of $V$, disintegrates into a spray and at the point of disintegration the ratio $V^2/r_0\gamma$ remained approximately constant [33]. Then Taylor [34] found that the critical angle of the meniscus which is called as "Taylor's cone" closed to disintegration is 49.3°. On the other hand Yarin et al. showed that Taylor's cone represents a specific self-similar solution while nonself-similar solutions that do not tend to the semivertical angle. The shape of the meniscus changes as the concentration of the polymer in solution and the solution viscosity increases [35]. Another work showed that conductivity of solution changes the shape of the meniscus. Various voltages have significant effects on droplet size, fiber diameter, and current transport. It has been verified experimentally that the shape of the initiating drop changes with applied voltage [36].

The shape of the surface changes significantly under a critical voltage. The surface changes and the electrospinning current, which significantly depends on voltage, increase in the bead formation, number of beads, and the defects on the surface of electrospun fiber web [37].

Lukas et al. analyzed the self-organization of the liquid jet [14]. In this analysis, it is supposed that electrohydrodynamics of a liquid surface can be analyzed with the capillary waves running on a one-dimensional approximation of the liquid surface, oriented along the horizontal axis, like *x-axis*, of a Cartesian system of coordinates. The critical electric strength $E_c$ for unstable waves that start to form cone was formulated as:

$$E_c = \sqrt[4]{\frac{4\gamma\rho g}{\varepsilon 2}} \tag{4}$$

where $\gamma$ is the linear force of surface tension, $\rho$ is the mass density of liquid, $g$ is the gravitational acceleration, $\varepsilon$ is the permittivity. The above assumption indicated that the critical electrical field strength, $E_c$, allows the creation of surface wave for initiating of jets.

From the previous work [31] it was found that upon increasing applied voltage the number of cones increases on the surface. As a result, fabric throughput increased. All these assumptions above are for needleless electrospinning. The minimum electric field depends on the surface tension and density of the solution, relative permittivity of the surrounding gas, and gravitational acceleration. As soon as the electric field increases and exceeds the critical electric field, a charged jet ejects from the apex of the cone and deposits on the collector.

*3.1.3. Distance between electrodes*

The distance between electrodes is another phenomenon that controls the final fiber diameter and morphology. Sufficient time to dry out the solvent from a polymer solution is necessary. If the distance between electrodes is too short, there is not enough time for drying, beaded, and sticky fiber structures can be observed. On the contrary, if the distance is too high, the electric field between electrodes decrease and forming of fiber is difficult.

Yuan et al. found that there were no obvious differences between the morphologies of the electrospun polysulfone (PSF) fibers at the 10–15 cm electrode to electrode distance. Increasing the collection distance could give more time for the solvent to evaporate and for the charged fluids to split more times [38]. The effect of the tip to collector distance on the fiber morphology is not as significant as that of other parameters, and this has been observed by many investigators [39–41].

*3.1.4. Ambient conditions*

Electrospinning is affected by an electric field. It means that any change in the electrospinning environment will affect the electrospinning process. When humidity is high, it is likely that water condenses on the surface of the fiber. At a very low humidity, a volatile solvent may dry out very rapidly. The evaporation of the solvent may be very fast. As a result, the electrospinning process may only be carried out for a few minutes before the needle tip is clogged. Many studies showed that ambient conditions (relative humidity, temperature) influence fiber diameter, morphology, and spinning performance [12].

*3.1.5. Velocity of rotating roller*

The main function of the roller consists in feeding the polymer solution from a tank in the form of solution layer on the roller surface into the electrospinning process between the spinning and collector electrode. The role of velocity of the rotating roller can be summarized as:

- Arrangement of the thickness of polymer solution layer on the surface of roller.

- Changing the feed rate of polymer solution [42] (**Figure 4**).

- The time available for formation Taylor's cones and the spinning process from these cones.

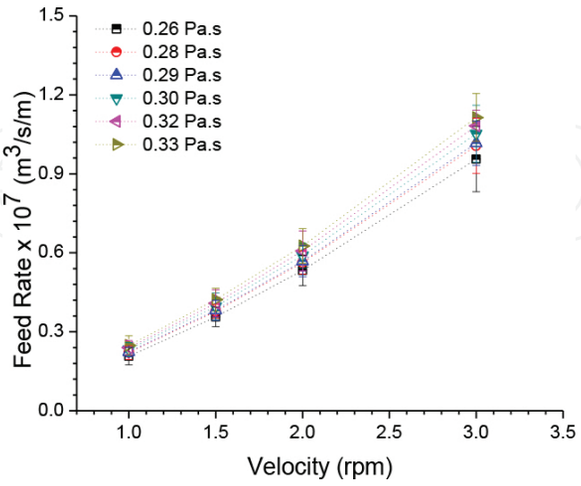


**Figure 4.** Feed rate of various PEO solution layers as a function of roller rpm and viscosity.

The speed of roller significantly influences the quality of the resultant nanofiber web, as shown in **Figure 5**:

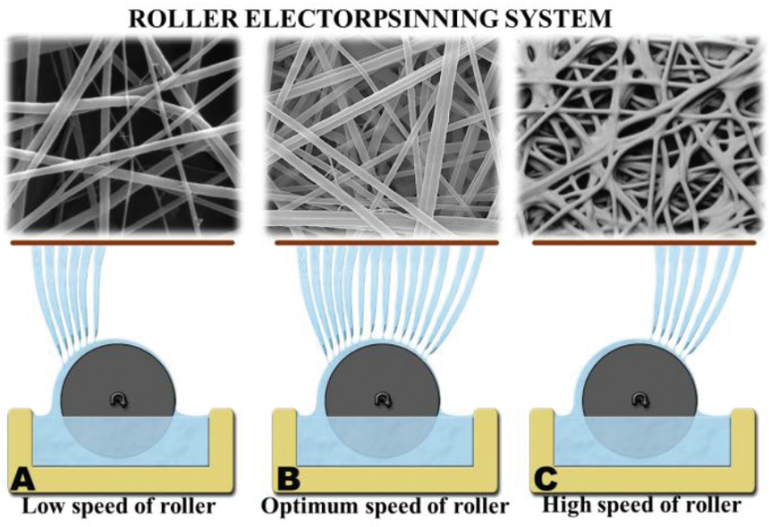


**Figure 5.** Effect of roller speeds on the quality of nanofiber web.

At the very low speed of roller (A), there will be not enough solution on the roller surface, so the number of cones forms on the roller surface and spinning performance will be very low. It is necessary to arrange roller speed as optimum (B) to get the best quality of nanofiber layer and high throughput. If the roller speed is very high (C), there might be a significant amount of solution supplied to the top of the roller, but there will be not enough time to form Taylor 's cones on the surface of the roller. The fiber quality will decrease.

*3.1.6. Velocity of take-up fabric*

During the roller electrospinning process, a supporting material (often a nonwoven fabric) is passing along the collector electrode to collect the fibers in the form of a more or less regular nanofiber layer on its surface. The speed of this fabric (in meters per minute) influences the area weight of a nanofiber layer and also affects the quality of nanofiber membrane, namely its regularity and nonfibrous area. The area weight of the resultant nanofiber layer can be easily calculated from the spinning performance and the velocity of supporting materials. Typical values of the velocity amount from 0.1 to 10 m/min.

*3.1.7. Geometry and conductivity of the collector electrode*

In the needleless ES, many jets are formed simultaneously on the surface of the spinning electrode. Jets are generated on the free liquid surface by a self-organizing process. Because of this, it is harder to control the spinning process when compared with the needle electrospinning process. The spinnerets in the needle electrospinning play an essential role in determining the product quality and productivity. Despite the success in needleless electrospinning, a design of a principle for a better needleless electrospinning process is still in progress. That is why the effort of scientists was focused on the shape of spinning electrodes.

Niu et al. [43] studied the influence of spinner shape on the electrospinning process using three rotating fiber generators, cylinder, disc, and coil. The electric field generated in the vicinity of these spinners was analyzed by a finite element method, and the calculations indicated that electric field intensities on these spinnerets are distributed differently. It was observed that, on the cylinder spinneret, the electrical field was distributed unevenly. The middle part of the cylinder spinneret had lower strength. Among all the spinneret, only the coil surface showed an intensity peak. In comparison of the cylinder and the needle electrospinning system, finer nanofibers with narrower fiber diameter distribution were produced by using coil and the disc spinneret. Compared to needle, cylinder, and disc electrospinning, higher productivity was achieved as 23 g/h using coil electrospinning.

The collector electrode in electrospinning is a conductive material. The collector can be directly connected to a high voltage supplier that gives the opposite charge than the spinning electrode has, or it can be grounded. Fibers that are collected on the nonconducting material usually have a lower packing density compared to those collected on a conductive surface.

### 3.2. Dependent parameters

*3.2.1. Number of cones*

Some Taylor's cones are simultaneously present on the spinning surface of the spinning roller electrode. Some cones ($N_c$) depend strongly on independent electrospinning parameters.

Cones were counted using a camera record as shown in **Figure 6** and their number is related to the spinning area determined from the same record [10].

The average number of cones ($N_c$) is counted from these pictures. The density of cones ($D$) can be calculated as the ratio of number of cones ($N$) to the spinning area ($A$).

$$D = N_c / A \left(1/m^2\right) \tag{5}$$

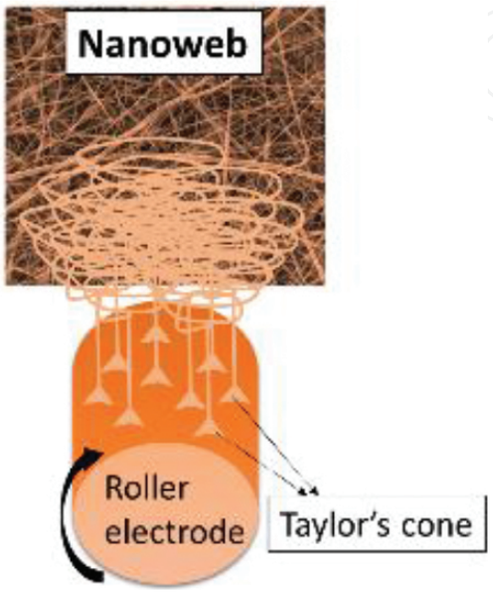


**Figure 6.** Number of cones on the roller surface.

*3.2.2. Spinning performance and spinning performance per jet*

Spinning performance (SP) is one of the most important characteristics of the nanofiber production process, influencing the production costs. The spinning performance of a single needle electrospinning is quite low while rather a high performance can be achieved by the needleless system. Spinning performance strongly depends on all the independent parameters and influences the quality of nanofibers as well as that of nanofiber layers.

SP can be determined from the mass of nanofibers produced in a 1 m long roller spinning electrode in 1 min. Spinning performance is calculated from area weight of produced nanofiber layer as follows:

$$\mathrm{SP} = \frac{GvL_f}{L_r} [\mathrm{g/min/m}] \tag{6}$$

where $G$ is the area weight of nanofibers membrane per area in g/m$^2$; $v$ is the velocity of running collected fabric, in m/min; $L_f$ is the width of nanofibers membrane on collected fabric, in m; and $L_r$ is the length of spinning roller, in m.

Spinning performance per one Taylor's cone (SPC) can be calculated from the known values of SP and an average total number of Taylor's cones on the spinning electrode $N_c$ using the camera images.

*3.2.3. Fiber diameter and fiber diameter distribution*

The fiber diameters are easily measured on the scanning electron microscope (SEM) microphotographs using software.

*3.2.4. Nonfibrous area*

The term nonfibrous area (**Figure 7**) was created as a measure of nanofiber layer quality which is a percentage of the area of an SEM microphotograph of nanofiber layer occupied by nonfibrous formations such as beads, foils, and so on.

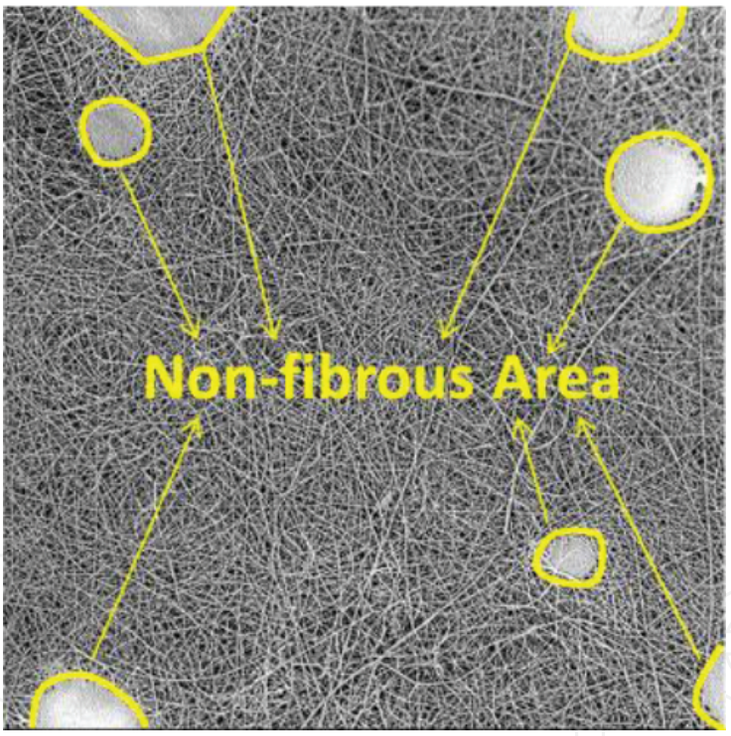


**Figure 7.** Nonfibrous area on the surface of nanofiber web.

*3.2.5. Lifetime of a jet*

A lifetime of a jet can be defined as the period from the point that the jet appears on the spinning electrode to the point that the jet disappears. The solution properties, roller speed, electric field strength, the number of cones, and the thickness of a layer on the roller surface are the main parameters that affect the lifetime of the jet. The lifetime of a jet can be measured using a camera

record of the spinning area during electrospinning. The measurement procedure consists in tracing a specific Taylor's cone during step-by-step playing the record.

*3.2.6. Average current and current per jet*

Under an electrostatic field, the polymer solution droplet becomes distorted by the induced electrical charge on the liquid surface, and a stable jet of the polymer solution is then ejected from the cone. The breakup of the jet depends on the magnitude of the applied electric current [10]. The bending instability in a charged jet was characterized by Reneker and Chun during electrospinning [44]. Many researchers on electrospraying have focused on the understanding of a current-voltage relationship. Previous attempts to correlate current with the electric field and flow rate suggested nonunique linear [45] or power law [46] dependencies. Using the power law, Fallahi et al. [47] showed that the relationship between current and voltage as current ~ $(\text{voltage})^{2.53}$. Demir et al. [48] reported a power law relationship between the solution flow rate ($Q$) and the applied voltage ($V$) with an exponent value of three in the experiments where $Q$ was not controlled. Bhattacharjee et al. [49] showed that current depends not only on applied voltage but also on conductivity and feed rate of the polymer solution. The relationship between current and other parameters was indicated that [49]

$$I \sim E^{*} Q^{0.5*} K^{0.4} \tag{7}$$

Theron et al. [46] reported that the average, electric current increased with the increase in the feed rate and voltage. It was also found that with increasing the applied voltage and solution conductivity both the jet current and fiber diameter were increased [47]. Because increasing the electric field increases the electrostatic stresses, which in turn, draws more material toward the collector. Kim et al. found that there is an optimum average electric current for the electrospinning process that depends on the solution properties [50]. Measurement of current per one jet was suggested in the previous work [13]. The strong relationship between the current of polymer solution jet and spinnability as well as spinning performance was demonstrated by Cengiz et al. using a rod electrospinning system. They found that electric current of the solution jet increases with the increasing concentrations of PU and TEAB, and current indicates the spinning performance [51].

*3.2.7. Thickness of polymer solution layer on the surface of the roller*

The effect of roller rotation on the thickness of polymer solution layer has been examined in several papers [52–54]. There have been several theoretical and experimental advances. Frenkel et al. investigated the nonlinear stability of a film flowing down a cylinder using the strong surface tension approximation and showed that wall curvature significantly influences the transverse disturbance of the film, suppressing harmonics of high angular frequency [53]. In a previous work, it was suggested the measurement of the thickness of layer on the surface of rotating roller using a custom-built micrometer, as shown in **Figure 8** [42]:

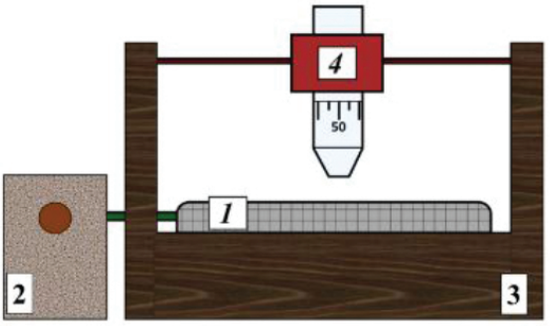


**Figure 8.** Number (1) is the rotating roller with a diameter of 20.0 mm driven by an electrical motor; (2) and (3) are the polymer solution tank; (4) is the micrometer.

The relationship between thicknesses of layers on the roller surface and roller speed is found proportional [42], as shown in **Figure 9**:

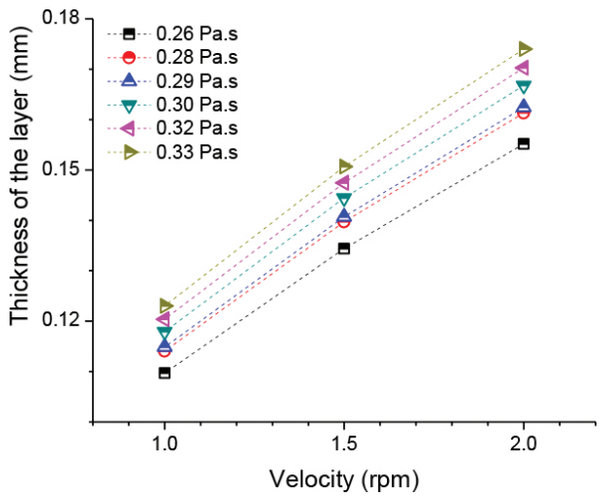


**Figure 9.** The thickness of various PEO solution layers as a function of roller rpm and viscosity.

### *3.2.8. Force acting on a jet*

The analysis and calculation of the force acting on a jet versus flow of polymer solution into this jet were performed during the spinning process. The Navier-Stoke equation model has been proposed to describe the force. Relations between the force acting on a jet and the volume flow rate $\dot{V}$, dynamic viscosity $\mu$ and thickness of the fluid layer $h$ were calculated in the literature [10, 55].

It seems to be tough to calculate the force acting on the jet based on the Coulomb's law as the electric field between the electrodes in the electrospinning device is certainly not static. Therefore, it was calculated the force from the volume flow rate, the thickness of polymer solution layer on the roller spinning electrode and the diameter of the base of Taylor's cone.

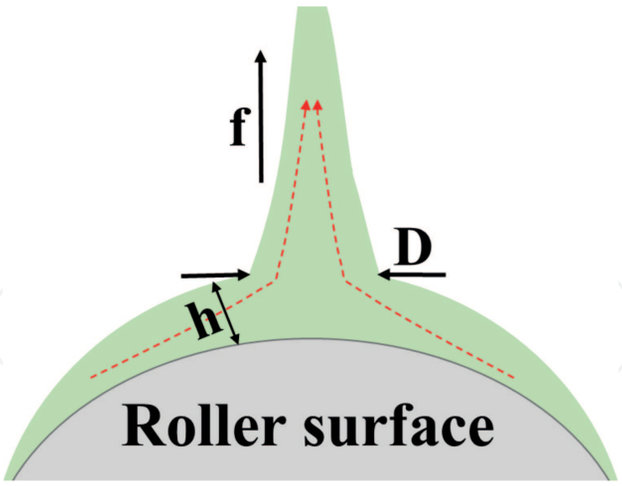


**Figure 10.** Schematic diagram of Taylor'scone. f—electric force, h—thickness of the fluid layer, D—diameter of the base of Taylor's cone.

The calculation relies on the idea that the polymer solution flows from the layer on the spinning roller into the jet through the circular area of radius $R$ and the height $h$ as shown in **Figure 10**. The flow is described using the Navier-Stokes equation as follows:

*3.2.8.1. Steady laminar stokes flow over a plate*

Full formulation of the momentum equations of the Navier-Stokes equation is:

$$\frac{\partial \mathbf{u}}{\partial \mathrm{t}} + \frac{\partial(\mathbf{uu})}{\partial \mathbf{x}} = \frac{\partial p}{\partial \mathbf{x}} + \mu \frac{\partial^2 \mathbf{u}}{\partial \mathbf{x}^2} + \boldsymbol{f} \tag{8}$$

Eq. (8) is rewritten in the form only for relevant direction $x$ and the first unsteady term is zero, the second term depicts nonlinear flow behavior, and it is zero, the pressure gradient is zero, the viscous term is partially neglected, external force remains and so the simplified equation after revision is as follows:

$$\mu \frac{\partial^2 u}{\partial y^2} = -f_y = -f \tag{9}$$

The next step is to find the velocity as a function of the *y-coordinate*, so Eq. (9) must be integrated and coefficients will be determined from the boundary conditions (b.c.) as follows:

$$\frac{\partial^2 u}{\partial y^2} = -\frac{f}{\mu} \tag{10}$$

$$\frac{\partial}{\partial y}\left(\frac{\partial u}{\partial y}\right) = -\frac{f}{\mu} \tag{11}$$

$$\left(\frac{\partial u}{\partial y}\right) = -\frac{f}{\mu}y + C_1 \cdots \quad b.c.: \cdots b.c.: y = h, \tau = \mu\frac{\partial u}{\partial y} = 0, \cdots \frac{\partial u}{\partial y} = 0 C_1 = \frac{f}{\mu}h \tag{12}$$

Note: the previous condition took account of the Newton fluid behavior. This place should be revised in the case of the non-Newtonian fluid. However, if non-Newtonian fluid will be still based on the velocity gradient, then this relation will be valid for non-Newton fluids as well.

$$\left(\frac{\partial u}{\partial y}\right) = -\frac{f}{\mu}y + \frac{f}{\mu}h \tag{13}$$

$$u(y) = -\frac{1}{2}\frac{f}{\mu}y^2 + \frac{f}{\mu}hy + C_2 \tag{14}$$

$$\text{b.c.: y} = 0, u = 0, \ldots C_2 = 0 \tag{15}$$

The velocity depends on the *y*-coordinate:

$$u(y) = -\frac{1}{2}\frac{f}{\mu}y^2 + \frac{f}{\mu}hy \tag{16}$$

After formal rewritten:

$$u(y) = \frac{1}{2}\frac{f}{\mu}\left[2hy - y^2\right] \tag{17}$$

Eq. (17) describes the velocity distribution on the *y*-coordinate so-called the velocity profile.

Mass flow rate:

$$\dot{Q} = \int_S u(y)\rho dS = \frac{1}{2}\pi D\rho\int_0^h \frac{f}{\mu}\left[2hy - y^2\right] \tag{18}$$

$$dy = \frac{\pi Df}{2\vartheta}\left[hy^2 - \frac{1}{3}y^3\right]_0^h = \frac{\pi Dfh^3}{3\vartheta} \tag{19}$$

where $\vartheta$ represents a kinematic viscosity in units $m^2/s$.

External local force per volume of the fluid is calculated from Eq. (19) and takes a form as follows,

$$f = \frac{3\dot{Q}\vartheta}{\pi Dh^3} = \frac{3\dot{V}\rho\mu}{\pi Dh^3\rho} = \frac{3\dot{V}\mu}{\pi Dh^3} \tag{20}$$

where $\dot{Q}$ is the mass flow rate (kg/s), $\dot{V}$ is the volume flow rate ($m^3/s$), $\vartheta$ is kinematic viscosity, and $\mu$ is dynamic viscosity, respectively.

The total force for the whole volume of the fluid in a Taylor cone is:

$$F = \int_V f dV = \int_0^{2\pi}\int_0^h\int_0^R frd\varphi dydr = \frac{3\dot{V}\mu}{2\pi h^3}\int_0^{2\pi}\int_0^h\int_0^R \frac{1}{r}rd\varphi dydr = \frac{3V\dot{\mu}R}{h^2}\left[\frac{\mathbf{kgm}}{\mathbf{s}^2}\right] \tag{21}$$

In fact, the force $F$ depends on electrical characteristics of the space between electrodes and on applied voltage. The quantities on the right side of Eq. (21) influence each other in such a manner that Eq. (21) remains true when any of these quantitiesis changed.

For instance, the increase in the thickness $h$ causes a corresponding increase of $V$ and/or $R$.

The influence of the fluid viscosity seems to be out of validity of Eq. (21). The growth of the solution viscosity depending on both polymer concentration and its molecular weight is linked with a greater degree of macromolecules entanglement and with the strength of jets that increases the volume flow rate. Above-mentioned relations make it rather difficult to study influences of specific parameters separately.

The results are a theoretical base for future experimental investigations. Nevertheless, some specific influences must be taken into account in planning and evaluation of the experiments which are discussed above [10, 55].

*3.2.9. Spinning area and the position of the jets*

The spinning area is the place where the Taylor's cones occur on the roller surface. The experimental results showed that the spinning area mainly depends on the parameters mentioned in **Table 1** such as speed of roller, polymer solution properties, electrical field, additives used in solution, and number of jets [10, 42]. The relationship between the spinning area and the position of jets was explained in Section 3.1.5 (**Figure 5**).

The thickness of a polymer solution layer on the roller influences the solution to flow into Taylor cones. Simultaneously, polymer solution, when moving out of the tank, needs a certain time to create Taylor's cones. Subsequently, the solution from the vicinity of Taylor's cones is dragged into the cones and following jets, being consumed gradually. If the velocity of the roller is slow, there is only a small amount of solution brought to the surface, and the solution is spun away before it reaches tank again. Thus, only a part of the potential spinning area is utilized. On the other hand, if roller velocity is too high, there is not enough time for a solution to create Taylor's cones and the spinning area is narrow again. The spinning area can be determined by using a camera.

*3.2.10. Distance between neighboring jets*

The average interjet distance is Describe dregarding wavelength ($\lambda$) as Lukáš et al. calculated it [15]. According to this formula, electric field strength, surface tension, density of the solution, the relative permittivity of the surrounding gas, and gravitational acceleration are the main parameters that affect the interjet distance [10]. In other studies [11, 42], the distance between neighboring jets was calculated using the number of jets ($n$) and spinning area ($A$). The spinning area $A$ is divided into $n$ identical squares belonging to Taylor's cones.

$$A = n.x^2 \tag{22}$$

$x(m)$ is the length of the square side (and simultaneously the distance between Taylor cones). Then the average distance $x$ between adjoining Taylor cones is

$$x = \sqrt{\frac{A}{n}}\,(\mathrm{m}) \tag{23}$$

*3.2.11. Length of the jet in stable zone*

The length of the jet of the polymer solution was described and studied by Dao [16]. The distance between the tip of a Taylor cone and the splitting point of a jet is called length of the jet. The long-range repulsive electrostatic forces between ions of the same sign cause the disintegration of charged jet body. If electric forces are stronger than the capillary forces, the jet will split or will be formed by the whipping instability. The process of concentration of ions at the surface of a jet preceding the onset of splitting or whipping instability is shown in **Figure 11** [10]. The condition of the process, such as solution viscosity, the amount of ions per volume unit, etc., predetermines the length of a jet.

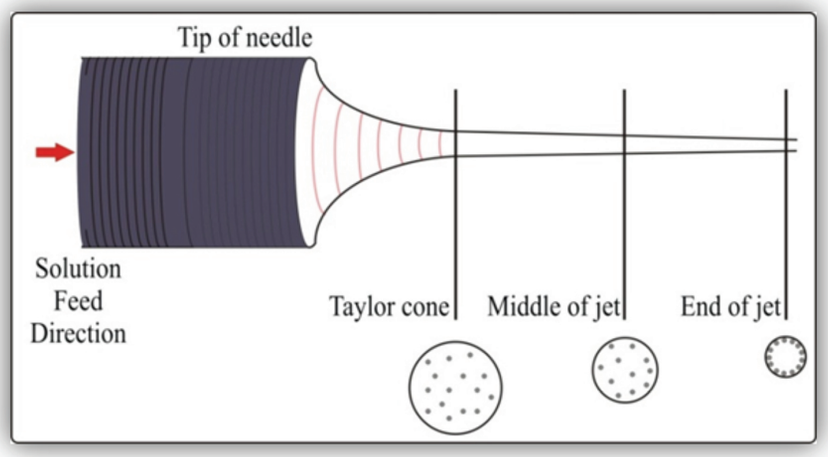


**Figure 11.** Radial movement of ions in a jet.

In the polymer solution entering the electrospinning process, the ions are more or less regularly distributed in the volume. When the stretching of a jet starts, the ions move toward the surface of the jet due to repulsive forces. As soon as the concentration of ions at the surface and the corresponding repulsion forces are big enough, the disintegration process starts. The viscosity and conductivity of solution are the key parameters influencing the time necessary for the onset of disintegration. If the viscosity is high, movement of ions toward the surface takes more time,and the length of the jet will be greater [16]. The addition of salt increases the conductivity of solution as well as a number of ions in the solution. If a number of ions are high, the time for ions to reach critical concentration will be shorter. Consequently, the jet will be shorter [16].

*3.2.12. Launching time of jet*

Highly concentrated solutions have an intensive entanglement of polymer chains. Therefore, coulombic repulsion force will not be sufficient to start jetting. However, the surface area has to be increased to accommodate the charge build-up on the jet surface which occurs through the formation of fibers. Deitzel et al. [56] suggested mobility of particles in electrospinning jet initiation to occur from the surface layers of the cone. The reason is partly due to surface shear forces generated by the potential difference between the electrodes.

The time needed for Taylor cone formation (characteristic hydrodynamic time) was experimentally determined from voltage-time oscilloscope records of the electrospinning onset event that were accompanied by video-records [57]. It was hypothesized that the characteristic hydrodynamic time is of the same order as the theoretically derived reciprocal value of the wave growth rate that is denoted here as "relaxation time." The derivation was based on the linear stability analysis. It was found that these times are of dynamic nature and hence they are viscosity dependent. The theoretical derivation of relaxation time for conductive viscous liquids was introduced and related to experimental measurements of characteristic hydrodynamic times. It was assumed that relaxation time $T$ is the reciprocal quantity to the growth factor $A$, $A = 1/T$.

$$A = -O_h K^2 + \sqrt{O_h^2 K^4 - \Omega_0^2} \tag{24}$$

where $\Omega_0^2$ is the dimensionless square of the angular frequency of a nonviscose liquid, $A$ is the dimensionless growth factor of a viscose liquid; $K$ is the dimensionless wavenumber and $O_h$ is the Ohnesorge number.

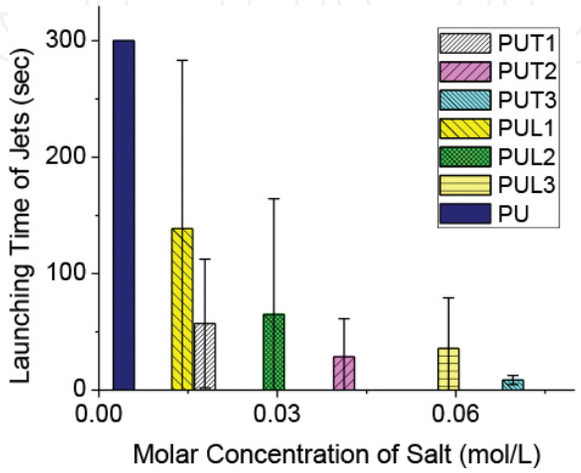


**Figure 12.** Launching time of jets according to the various molar ratio of tetra ethylene ammonium bromide (T) and lithium chloride (L) content of salts in polyurethane (PU) solution.

Recently, it was suggested the measurement of launching time by observing and recording the timing. The results indicated that additives have asignificant influence on the launching of jets as shown in **Figure 12** [10].

Additional salt increases the conductivity of the solution. The charged solution can easily influence from the electrical field between the electrodes and yields to form Taylor's cone.

## 4. Conclusion

A needleless electrospinning system is a significant method for the industrial production. Compared to the needle electrospinning system, there still requires more work to define the parameters and measurement methods of parameters. This chapter summarizes the parameters of needleless electrospinning. First, parameters grouped as dependent and independent parameters. Then, the relationship between parameters is defined, and the measurement methods were introduced systematically. The results can be concluded that:

- The total electric current in the roller electrospinning is more or less proportional to the spinning performance. On the contrary, the current per jet is not commensurate with the spinning performance per jet. This discrepancy evoked a more thorough investigation of the phenomena. The results were separately published [11] and are not a part of this chapter;

- The relationship between the number of jets and the spinning performance on the roller velocity is generally nonmonotonous. The main influence factors for the relation are the thickness of solution layer and feed rate versus movability of jets against the roller surface [10, 42];
- The launching time of jets does not influence the number of jets on the spinning roller and spinning performance significantly. It only can affect the starting period of the spinning process. As soon as the spinning process becomes stable, the number of jets depends on other parameters and is principally stable;
- The experimentally found distance between jets is in a reasonably good agreement with theoretical conclusions of Lukas. Nevertheless, it depends on some more variables than Lukas considered, namely on the conductivity of polymer solution;
- The spinning area mainly depends on the movement of the roller. Experimental results of PEO showed that increasing roller rpm decreases the spinning area except PEO without salt. The relationship between the spinning area and spinning performance is related to the number of jets. The higher number of jets means the larger spinning area which also means higher SP [42];
- The length of jets mainly depends on the amount of salt which is related to conductivity and the viscosity of the solution. Experiments showed that there is no relation between SP and length of jets [10];
- The effect of the rotating roller on fiber surface morphology indicates that increasing roller speed increase the fiber diameter and nonfibrous area. It is necessary to optimize roller speed to obtain proper fiber diameter and minimum nonfibrous area for every polymer solution [10, 42];
- The salts may influence the entanglement number and polarity of macromolecules when creating complex bonds with them. On the other hand, the salts increase the conductivity of solutions which may cross the limits supposed by the model of a "leaky dielectric."

The role of all parameters is important for better productivity of nanofibers in fine diameter.

## Author details

Fatma Yalcinkaya[1*], Baturalp Yalcinkaya[1] and Oldrich Jirsak[2]

*Address all correspondence to: yenertex@hotmail.com

1 Institute for Nanomaterials, Advanced Technology, and Innovation, Technical University of Liberec, Liberec, Czech Republic

2 Department of Nonwovens and Nanofibrous Materials, Faculty of Textile Engineering, Technical University of Liberec, Liberec, Czech Republic

## References


[1] Vasita, R. and D.S. Katti, *Nanofibers and their applications in tissue engineering*. International Journal of Nanomedicine, 2006. 1(1): pp. 15–30.

[2] Xue, J.J., et al., *Drug loaded homogeneous electrospun PCL/gelatin hybrid nanofiber structures for anti-infective tissue regeneration membranes*. Biomaterials, 2014. 35(34): pp. 9395–9405.

[3] Heo, D.N., et al., *Burn-wound healing effect of gelatin/polyurethane nanofiber scaffold containing silver-sulfadiazine*. Journal of Biomedical Nanotechnology, 2013. 9(3): pp. 511–515.

[4] Yalcin, I., et al., *Design of polycaprolactone vascular grafts*. Journal of Industrial Textiles, 2016. 45(5): pp. 813–833.

[5] Niu, H.T. and T. Lin, *Fiber generators in needleless electrospinning*. Journal of Nanomaterials, 2012. 2012: p. 13.

[6] Jirsak, O., et al., *A Method of Nanofibers Production from a Polymer Solution Using Electrostatic Spinning and a Device for Carrying Out the Method*, in *EP1673493*. 2005: Czech Republic.

[7] Cengiz, F. and O. Jirsak, *The effect of salt on the roller electrospinning of polyurethane nanofibers*. Fibers and Polymers, 2009. 10(2): pp. 177–184.

[8] Yener, F., et al., *New measurement methods for studying of mechanism of roller electrospinning*. Nanocon 2013, 5th International Conference, 5th–7th November 2014, Czech Republic: pp. 808–813.

[9] Dao, A.T., O. Jirsak, and T. Ltd, *Roller electrospinning in various ambient parameters*. Nanocon 2010, 2nd International Conference, 2010: pp. 103–108.

[10] Yener, F., *New methods in the study of roller electrospinning mechanism*, in *Department of Nonwoven and Nanofibrous Materials*. 2014, Technical University of Liberec: Liberec. p. 136.

[11] Yener, F., B. Yalcinkaya, and O. Jirsak, *On the Measured current in needle- and needleless electrospinning*. Journal of Nanoscience and Nanotechnology, 2013. 13(7): pp. 4672–4679.

[12] Tonks, L., *A Theory of liquid surface rupture by a uniform electric field*. Physical Review, 1935. 48(6): pp. 562–568.

[13] Landau, L.D., Course of Theoretical Physics; v. 8., E.M. Lifshitz, Editor. 1960, Oxford: Reading, Mass: Pergamon Press; Addison-Wesley (*Electrodynamics of Continuous Media/by L.D. Landau and E.M. Lifshitz; translated from the Russian by J.B. Skyes and J.S. Bell*.).

[14] Lukas, D., A. Sarkar, and P. Pokorny, *Self-organization of jets in electrospinning from free liquid surface: ageneralized approach*. Journal of Applied Physics, 2008. 103(8) pp. 084309–1–084309–7.

[15] Lukáš, D., et al., *Physical principles of electrospinning (Electrospinning as a nano-scale technology of the twenty-first century)*. Textile Progress, 2009. 41(2): 59–140.

[16] Dao, A.T., *The Role of Rheological Properties of Polymer Solutions in Needleless Electrostatic Spinning*, in *PhD. thesis*. 2010, Technical University of Liberec: Liberec. p. 80.

[17] Yalcinkaya, F., et al., *Preparation of antibacterial nanofibre/nanoparticle covered composite yarns*. Journal of Nanomaterials, 2016. 2016(4): p. 7.

[18] Shenoy, S.L., et al., *Role of chain entanglements on fiber formation during electrospinning of polymer solutions: good solvent, non-specific polymer-polymer interaction limit*. Polymer, 2005. 46(10): pp. 3372–3384.

[19] McKinley, G.H. and T. Sridhar, *Filament-stretching rheometry*. Annual Review of Fluid Mechanics, 2002. 34: pp. 375–415.

[20] Barnes, H.A., *A Handbook of Elementary Rheology, University of Wales Institute of Non-Newtonian Fluid Mechanics*. 2000, University of Wales, Institute of Non-Newtonian Fluid Mechanics, Aberystwyth.

[21] Kim, K.W., et al., *The effect of molecular weight and the linear velocity of drum surface on the properties of electrospun poly(ethylene terephthalate) nonwovens*. Fibers and Polymers, 2004. 5(2): pp. 122–127.

[22] Buchko, C.J., et al., *Processing and microstructural characterization of porous biocompatible protein polymer thin films*. Polymer, 1999. 40(26): pp. 7397–7407.

[23] Mit-uppatham, C., M. Nithitanakul, and P. Supaphol, *Ultrafine electrospun polyamide-6 fibers: effect of solution conditions on morphology and average fiber diameter*. Macromolecular Chemistry and Physics, 2004. 205(17): pp. 2327–2338.

[24] Cengiz, F., T.A. Dao, and O. Jirsak, *Influence of solution properties on the roller electrospinning of poly(vinyl alcohol)*. Polymer Engineering & Science, 2010. 50(5): pp. 936–943.

[25] Fong, H., I. Chun, and D.H. Reneker, *Beaded nanofibers formed during electrospinning*. Polymer, 1999. 40(16): pp. 4585–4592.

[26] Filatov, Y., A. Budyka, and V. Kirichenko, *Electrospinning of Micro-and-Nanofibers: Fundementals and Applications in Seperation and Filtration Process*. 2007. Bgell House Inc. Danbury, Connecticut, United states.

[27] Kim, S.J., C.K. Lee, and S.I. Kim, *Effect of ionic salts on the processing of poly(2acrylamido-2-methyl-1-propane sulfortic acid) nanofibers*. Journal of Applied Polymer Science, 2005. 96(4): pp. 1388–1393.

[28] Heikkila, P. and A. Harlin, *Electrospinning of polyacrylonitrile (PAN) solution: effect of conductive additive and filler on the process*. Express Polymer Letters, 2009. 3(7): pp. 437–445.

[29] Yener, F. and O. Jirsak. *Improving Performance of Polyvinyl Butyral Electrospinning*. in *3rd International Conference on Nanocon*. TANGER LTD 2011. Brno, Czech Republic.

[30] Yener, F. and O. Jirsak, *Comparison between the Needle and Roller Electrospinning of Polyvinylbutyral*. Journal of Nanomaterials, 2012. 2012: p. 6.

[31] Yener, F. and O. Jirsak. *Development of New Methods for Study of Mechanism of Electrospinning*. in *Workshop*. 2012. Světlanka: Technical University of Liberec.

[32] Melcher, J.R. and G.I. Taylor, *Electrohydrodynamics—a review of role of interfacial shear stresses*. Annual Review of Fluid Mechanics, 1969. 1: pp. 111–146.

[33] Zeleny, J., *Instability of electrified liquid surfaces*. Physical Review, 1917. 10: pp. 1–6.

[34] Taylor, G.I., *Disintegration of water drops in an electric field*. Proceedings of the Royal Society A: Mathematical, Physical and Engineering Sciences, 1964. 280: pp. 383–397.

[35] Yarin, A.L., S. Koombhongse, and D.H. Reneker, *Taylor cone and jetting from liquid droplets in electrospinning of nanofibers*. Journal of Applied Physics, 2001. 90(9): pp. 4836–4846.

[36] Baumgart,P.K., *Electrostatic spinning of acrylic microfibers*. Journal of Colloid and Interface Science, 1971. 36(1): pp. 71–79.

[37] Deitzel, J.M., et al., *The effect of processing variables on the morphology of electrospun nanofibers and textiles*. Polymer, 2001. 42(1): pp. 261–272.

[38] Yuan, X.Y., et al., *Morphology of ultrafine polysulfone fibers prepared by electrospinning*. Polymer International, 2004. 53(11): pp. 1704–1710.

[39] Geng, X.Y., O.H. Kwon, and J.H. Jang, *Electrospinning of chitosan dissolved in concentrated acetic acid solution*. Biomaterials, 2005. 26(27): pp. 5427–5432.

[40] Zhao, Z.Z., et al., *Preparation and properties of electrospun poly(vinylidene fluoride) membranes*. Journal of Applied Polymer Science, 2005. 97(2): pp. 466–474.

[41] Zhang, C.X., et al., *Study on morphology of electrospun poly(vinyl alcohol) mats*. European Polymer Journal, 2005. 41(3): pp. 423–432.

[42] Yalcinkaya, F., B. Yalcinkaya, and O. Jirsak, *Analysis of the effects of rotating roller speed on a roller electrospinning system*. Textile Research Journal, 2016 doi: 10.1177/0040517516641362.

[43] Niu, H.T., X.G. Wang, and T. Lin, *Upward needleless electrospinning of nanofibers*. Journal of Engineered Fibers and Fabrics, 2012. 7: pp. 17–22.

[44] Reneker, D.H. and I. Chun, *Nanometre diameter fibres of polymer, produced by electrospinning*. Nanotechnology, 1996. 7(3): pp. 216–223.

[45] Shin, Y.M., et al., *Experimental characterization of electrospinning: the electrically forced jet and instabilities*. Polymer, 2001. 42(25): pp. 9955–9967.

[46] Theron, S.A., E. Zussman, and A.L. Yarin, *Experimental investigation of the governing parameters in the electrospinning of polymer solutions*. Polymer, 2004. 45(6): pp. 2017–2030.

[47] Fallahi, D., et al., *Effects of feed rate and solution conductivity on jet current and fiber diameter in electrospinning of polyacrylonitrile solutions*. E-Polymers, 2009. 9: pp. 1250–1257.

[48] Demir, M.M., et al., *Electrospinning of polyurethane fibers*. Polymer, 2002. 43(11): pp. 3303–3309.

[49] Bhattacharjee, P.K., et al., *On the measured current in electrospinning*. Journal of Applied Physics, 2010. 107(4): pp. 044306–1–044306–7.

[50] Kim, S.J., K.M. Shin, and S.I. Kim, *The effect of electric current on the processing of nanofibers formed from poly(2-acrylamido-2-methyl-1-propane sulfonic acid)*. Scripta Materialia, 2004. 51(1): pp. 31–35.

[51] Cengiz-Çallioğlu, F., O. Jirsak, and M. Dayik, *Electric current in polymer solution jet and spinnability in the needleless electrospinning process*. Fibers and Polymers, 2012. 13(10): pp. 1266–1271.

[52] Khumalo, M.B. and O. Jirsak, *Roller Electrospinning with Regards to Roller Movement*, in *MSc. Thesis, Nonwoven Dept*. 2012, Technical University of Liberec: Liberec. p. 60.

[53] Frenkel, A.L., et al., *Annular flows can keep unstable films from breakup-nonlinear saturation of capillary instability*. Journal of Colloid and Interface Science, 1987. 115(1): pp. 225–233.

[54] Campanella, O.H. and R.L. Cerro, *Viscous-flow on the outside of a horizontal rotating cylinder-the roll coating regime with a single fluid*. Chemical Engineering Science, 1984. 39(10): pp. 1443–1449.

[55] Jirsak, O., K. Frana, and F. Yener, *Electrospinning Studies: Jet Forming Force*, in *Strutex*, Faculty of Textile engineering. 2012. Liberec. p. 97.

[56] Deitzel, J.M., et al., *Key parameters influencing the onset and maintenance of the electrospinning jet*. Polymeric Nanofibers, 2006. 918: pp. 56–73.

[57] Deliu, R., et al., *Needleless electrospinning relaxation time of the aqueous solutions of poly (vinyl alcohol)*. Materiale Plastice, 2014. 51(1): pp. 62–66.

IntechOpen